

Highly deformed high-spin band in ^{125}I

Purnima Singh, Somnath Nag, and A. K. Singh

Department of Physics & Meteorology, Indian Institute of Technology Kharagpur, Kharagpur, IN-721302, India

I. Ragnarsson

Department of Mathematical Physics, Lund Institute of Technology, Box 118, S-221 Lund, Sweden

H. Hübel, A. Al-Khatib, P. Bringel, C. Engelhardt, and A. Neußer-Neffgen

Helmholtz-Institut für Strahlen- und Kernphysik, Universität Bonn, Nussallee 14-16, D-53115 Bonn, Germany

G. B. Hagemann, C. R. Hansen, B. Herskind, and G. Sletten

Niels Bohr Institute, Blegdamsvej 17, DK-2100 Copenhagen Ø, Denmark

A. Bracco, G. Benzoni, and F. Camera

Dipartimento di Fisica, Università di Milano and INFN, Sezione di Milano, I-20133 Milano, Italy

P. Fallon and R. M. Clark

Nuclear Science Division, Lawrence Berkeley National Laboratory, Berkeley, California 94720, USA

M. P. Carpenter, R. V. F. Janssens, T. L. Khoo, and T. Lauritsen

Physics Division, Argonne National Laboratory, Argonne, Illinois 60439, USA

P. Chowdhury

Department of Physics, University of Massachusetts Lowell, Lowell, Massachusetts 01854, USA

H. Amro

Department of Radiation Oncology, University of Michigan, Ann Arbor, Michigan 48109, USA

(Received 14 March 2011; published 22 August 2011)

High-spin states in ^{125}I have been investigated using the reaction $^{82}\text{Se}(^{48}\text{Ca}, p4n)$ at a beam energy of 200 MeV and γ -ray coincidence events were detected using the Gammasphere spectrometer. A deformed rotational band, extending up to $I^\pi = 95/2^-$, was observed for the first time in a heavier odd- A iodine nucleus. The characteristics of the band are very similar to those of the highly deformed bands observed recently in neighboring nuclei and it is essentially identical to one of the previously known bands in ^{126}Xe . The experimental results are compared to cranked Nilsson-Strutinsky calculations and possible configurations for the band are discussed.

DOI: [10.1103/PhysRevC.84.024316](https://doi.org/10.1103/PhysRevC.84.024316)

PACS number(s): 23.20.Lv, 23.20.En, 27.60.+j, 21.60.Ev

I. INTRODUCTION

The generation of angular momentum in nuclei is a key question in nuclear structure physics. Within the framework of the single-particle model, it is due to alignment of the individual angular momenta of the nucleons available in the valence space, whereas within the collective model coherent motion of many nucleons is assumed. Nuclei with a few nucleons outside a closed shell represent ideal cases to explore the interplay between these competing mechanisms and the transition from noncollective to collective behavior or vice versa.

In the $A = 125$ mass region, noncollective maximally aligned states have been observed in ^{121}I [1], ^{125}I [2], ^{124}Xe [3], ^{123}Cs [4], and tentatively in ^{124}Ba [5], where all particles outside the $^{114}_{50}\text{Sn}_{64}$ core align their angular momenta along the same axis to generate terminating states. Furthermore, noncollective states above these terminating states have been

observed. They are the result of promoting neutrons from the $N = 64$ core to higher-lying orbitals [4].

The occurrence of rotational bands in the $Z = 49$ –54 nuclei in the mass-110 region has been attributed to two-particle-two-hole (2p-2h) excitations from the up-sloping proton $g_{9/2}$ orbitals across the $Z = 50$ shell closure. These collective structures are associated with a prolate minimum in the potential energy surface at $\epsilon_2 \simeq 0.25$ [6–12]. Most of these bands represent examples of so-called smooth band termination [13,14], where the collectivity decreases gradually with increasing spin. One of the bands in ^{113}I has tentatively been assigned a configuration involving the neutron $i_{13/2}$ intruder orbital originating from the $N = 6$ subshell [10]. However, no such band has been observed in the heavier I nuclei with $A > 121$. Furthermore, in the mass-130 region, the superdeformed (SD) bands observed in Ce nuclei [15–17] originate from neutron excitations across the $N = 82$ shell gap into $h_{9/2}$ and $i_{13/2}$ orbitals, coupled to the proton 2p-2h

excitation mentioned above [18]. Deformation parameters $\epsilon_2 \simeq 0.4$ have been determined for these SD bands [19].

The nuclei of the mass-125 region lie between the near-spherical nuclei with $A \simeq 110$ and the highly deformed and SD nuclei of the $A = 130$ region and, thus, have the potential of providing further insight into the development of collectivity.

Recent spectroscopic studies of nuclei with neutron number $N \simeq 70$, ^{124}Ba [5], ^{125}Xe [20], and ^{126}Xe [21], revealed deformed bands with remarkable regularity extending into the spin $I = 50$ –60 region. They feed normal-deformed states in the spin range $I = 22$ –25 at excitation energies around 10 MeV. Transition quadrupole moments of $Q_t \simeq 5.5$ b have been determined for several of these bands using a centroid-shift method, which corresponds to a deformation parameter of $\epsilon_2 \simeq 0.30$ [20,21]. It was suggested that these bands involve one or two neutrons in deformation-driving neutron $i_{13/2}$ intruder orbitals and, possibly, even a neutron in a $j_{15/2}$ orbital.

An interesting question, which requires further investigation, is whether the collectivity at high spin is only due to $N = 82$ core excitations or whether $Z = 50$ core excitations are important as well. It is, therefore, important to extend such studies to other nuclei of the mass-125 region.

In the present work, a spectroscopic investigation to search for deformed high-spin bands in ^{125}I using the Gammasphere spectrometer [22] is described. A regular band which extends up to $I^\pi = 95/2^-$ was discovered. It is essentially identical to one of the high-spin bands in ^{126}Xe [21]. Several states with maximally aligned and anti-aligned configurations have also been observed in this nucleus, and a one-to-one correspondence with results of cranked Nilsson-Strutinsky (CNS) calculations was found for those levels. These results were reported in a previous article [2].

In Sec. II the experimental procedure and the data analysis are described. In the subsequent section the new rotational band in ^{125}I is presented and in the last section the configuration assignment to this band, based on CNS calculations, is discussed.

II. EXPERIMENTAL PROCEDURE AND DATA ANALYSIS

Details on the experimental procedure have been presented in previous articles [2,21]. In short, high-spin states in ^{125}I were populated using the heavy-ion fusion-evaporation reaction $^{82}\text{Se}(^{48}\text{Ca}, p4n)^{125}\text{I}$. The ^{48}Ca beam with an energy of 205 MeV and an intensity of 4 pnA was provided by the ATLAS accelerator at Argonne National Laboratory. The target consisted of a 0.5 mg/cm^2 , 98.8% enriched, ^{82}Se layer evaporated on a 0.5 mg/cm^2 Au backing. The Se was protected by a 0.08 mg/cm^2 Au layer. The Au backing faced the beam and, hence, the beam energy at mid-target was about 200 MeV. Gamma-ray coincidence events were measured with the Gammasphere spectrometer [22], which consisted of 100 Compton-suppressed Ge detectors at the time of the experiment. In a beam time of seven days, a total of 2.8×10^9 events with a Ge-detector coincidence fold $f \geq 5$ were collected and stored on magnetic tape.

For the off-line analysis, the calibrated and gain-matched data were sorted into three- and four-dimensional arrays using the software package RADWARE [23]. To determine the multipolarity of γ -ray transitions, two angular correlation matrices were sorted. The first one contained events detected at forward and backward angles, close to average angles of 35° and 145° , respectively, on one axis and those registered in all detectors on the other axis. Similarly, the second matrix contained events detected around 90° on one axis and those of all detectors on the other axis. Coincidence gates were set in these matrices on the axis with events detected in all detectors. The intensity ratios $R_\theta = I(\gamma_2^{fb}, \gamma_1^{all})/I(\gamma_2^{90}, \gamma_1^{all})$ were around 0.6 and 1.2 for stretched dipole and stretched quadrupole transitions, respectively.

III. NEW HIGH-SPIN BAND

A partial level scheme, based on our previous work [2] and on the present results, is displayed in Fig. 1. The new high-spin rotational-like sequence, band 6, consists of eleven high-energy γ -ray transitions in cascade. In Fig. 2, the triple-gated γ -ray coincidence spectrum presented shows transitions of band 6 as well as γ rays from the previously known band 5 in ^{125}I [2].

Band 6 is linked via the 1054-keV transition to the $47/2^-$ level at 8042 keV of band 5. Figure 3 demonstrates the connection between the bands. This triple-coincidence spectrum, gated on all transitions of band 5 up to the $39/2^-$ state and, in addition, on the lines at 380 (band 5) and 1119 (band 6) keV, clearly shows the 1054- and 1075-keV peaks. The possibility of another linking transition with an energy of 1157 keV from the $55/2^-$ state of band 6 to the $51/2^-$ level of band 5 could not be established firmly due to the presence of the intense 1159-keV γ -ray transition of band 5.

The angular distribution ratio of $R_\theta = 1.06(12)$ measured for the 1054-keV transition is consistent with a stretched $E2$ character. Therefore, negative parity has been assigned to band 6. The R_θ ratios measured for the 1119-, 1191-, 1271-, 1365-, and 1472-keV γ rays from the lower part of the band are 1.05(10), 1.41(23), 1.24(18), 1.44(28), and 1.18(20), respectively. These values are consistent with quadrupole, most likely $E2$, multipolarity. For the higher-spin transitions no angular distribution ratios could be determined and $E2$ multipolarity is assumed since they form a smooth continuation of the sequence. The new band extends the level scheme of ^{125}I up to an excitation energy of 27 MeV and a spin and parity of $I^\pi = 95/2^-$.

IV. DISCUSSION

The new band 6 in ^{125}I exhibits characteristics similar to those of the regular high-spin bands discovered recently in ^{124}Ba [5], ^{125}Xe [20], and ^{126}Xe [21]. In particular, band 6 is almost identical to band a in ^{126}Xe . The difference between the average energies of two consecutive γ -ray transitions of band 6 and those of band a at approximately the same spin decreases from 14 keV at lower spin to 2 keV at high spin. The dynamic moments of inertia of these two bands are compared

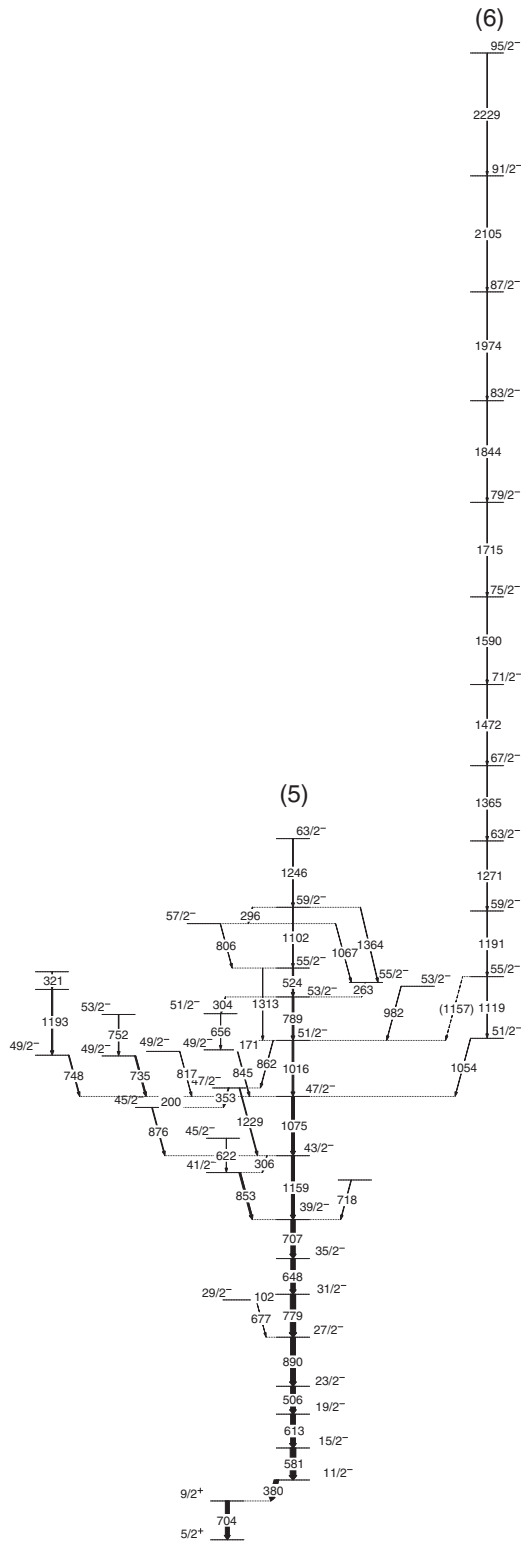


FIG. 1. Partial level scheme of ^{125}I , based on the present work and on previous results [2].

in Fig. 4. They decrease with increasing rotational frequency up to ≈ 0.8 MeV and then remain approximately constant. The irregularity observed at low frequency in band a of ^{126}Xe results from mixing of close-lying levels, and the irregular pattern around $\hbar\omega = 1.2$ MeV is due to a sudden gain in

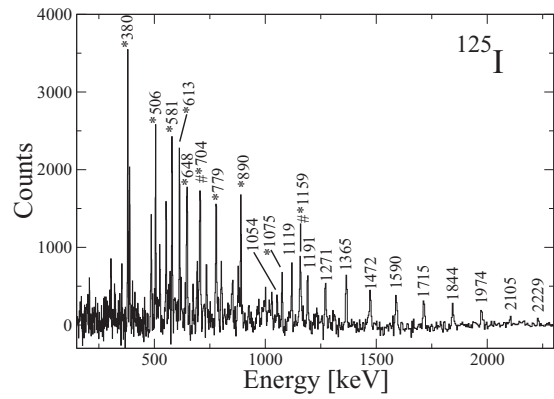


FIG. 2. Summed triple-gated γ -ray coincidence spectrum of band 6 in ^{125}I . The peaks marked with asterisks belong to low-lying yrast states. Peaks marked with hash marks are unresolved doublets.

alignment. The new band in ^{125}I could not be extended into this frequency range. The aligned angular momenta for the two bands are compared in Fig. 5. The alignment of band 6 in ^{125}I is, on average, $0.6 \hbar$ higher than that of band a in ^{126}Xe . This difference presumably results from the unpaired proton in ^{125}I . The close similarity of the two bands suggests that they are associated with the same intrinsic structure, where the additional proton in ^{126}Xe contributes with a negative alignment.

In order to understand the intrinsic structure of band 6, theoretical calculations were carried out within the framework of the configuration-dependent CNS formalism [14,24–26]. These calculations allow us to distinguish between single-particle orbitals with the main amplitude in different groups of j shells (i.e., either in a high- j intruder shell or distributed over the other j shells within an N shell). Fixed configurations can be traced as a function of spin all the way up to their termination in fully aligned states. The calculations are carried out on a mesh in the deformation space, $(\epsilon_2, \epsilon_4, \gamma)$. Then, for each fixed configuration and each spin separately, the total energy of the nucleus is determined by a minimization in the

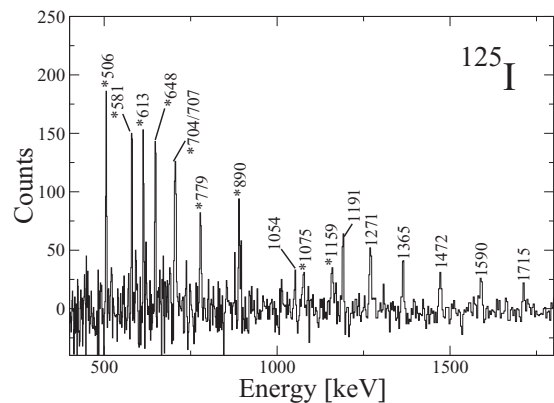


FIG. 3. Summed triple-gated γ -ray coincidence spectrum demonstrating the link between bands 5 and 6 in ^{125}I . The spectrum was obtained with a gate list of all transitions of band 5 up to the $39/2^-$ state and gates on the lines at 380 and 1119 keV. The peaks marked with asterisks belong to low-lying yrast states.

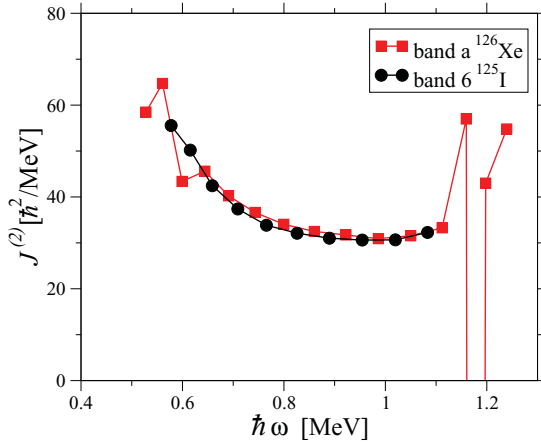


FIG. 4. (Color online) Dynamic moments of inertia $J^{(2)}$ as a function of rotational frequency for band 6 in ^{125}I and band a of ^{126}Xe [21].

shape degrees of freedom. Pairing correlations are neglected, which implies that the results are mainly relevant for high spins; i.e., for $I > 20$ –30 in this mass region. For the κ and μ parameters defining the $l \cdot s$ and l^2 strengths of the modified oscillator potential, the so-called $A = 110$ parameters [27] were used. These are known to give a good description of the smooth terminating bands in the neutron-deficient $Z = 49$ –54 nuclei [14]. The Lublin-Strasbourg drop model [28] is used for the macroscopic energy, with the rigid-body moment of inertia calculated with a radius parameter $r_0 = 1.16$ fm and a diffuseness parameter $a = 0.6$ fm [26].

Potential energy surfaces were calculated as a function of angular momentum for parity and signature $(\pi, \alpha) = (-, 1)$ for ^{125}I . They are displayed for the $I^\pi = 39/2^-$ – $75/2^-$ range in Fig. 6. The lowest minima correspond to oblate states ($\gamma = 60^\circ$), and they are competitive in energy up to very high spin. These states have been observed in ^{125}I at spin 39/2, 51/2, and 63/2 and are discussed in our previous publication [2]. In addition, several local minima occur. The minimum at $\varepsilon_2 \simeq 0.32$, $\gamma \simeq 5^\circ$ was previously associated with the configuration of band a in ^{126}Xe and with other high-spin bands on the basis

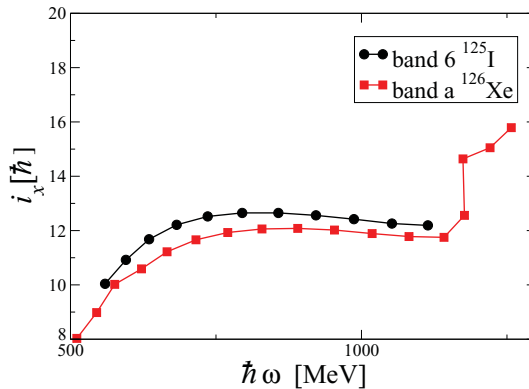


FIG. 5. (Color online) Aligned angular momenta as a function of rotational frequency for band 6 in ^{125}I and band a in ^{126}Xe relative to a reference with Harris parameters $J_0 = 30\hbar^2/\text{MeV}$ and $J_1 = 1\hbar^4/\text{MeV}^3$.

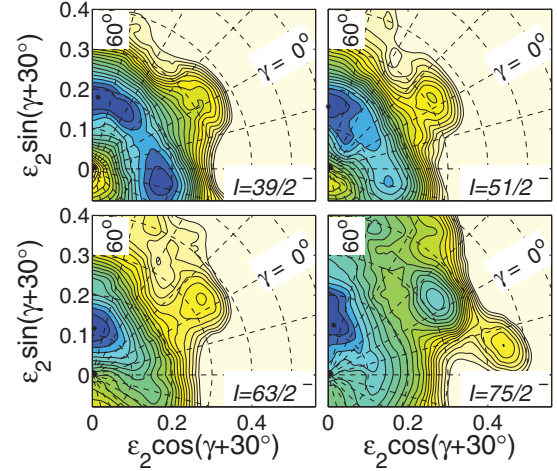


FIG. 6. (Color online) Calculated potential energy surfaces for ^{125}I with parity and signature $(\pi, \alpha) = (-, 1)$ in the spin range $I^\pi = 39/2^-$ – $75/2^-$. The contour-line separation is 0.25 MeV.

of the measured transition quadrupole moments [20,21]. It is very likely also relevant for the new band 6 in ^{125}I .

Calculations have then been carried out to search for configurations that correspond to this minimum. The configurations are labeled relative to the ^{100}Sn core by the shorthand notation $[p_1 p_2, n_1(n_2 n_3)]$, which stands for $\pi[(g_{9/2})^{-p_1}(h_{11/2})^{p_2}] \otimes \nu[(h_{11/2})^{n_1}(f_{7/2}, h_{9/2})^{n_2}(i_{13/2})^{n_3}]$, with the remaining particles (protons and neutrons) outside the core located in the mixed $d_{5/2}$, $g_{7/2}$, $s_{1/2}$, and $d_{3/2}$ orbitals.

The results of the calculations for six low-energy configurations with $(\pi, \alpha) = (-, 1)$ are presented in Fig. 7. The excitation energies are plotted relative to the rotating liquid drop energy [26] as a function of spin. For comparison, the [21,6(00)] configuration is included. It is less collective and terminates in an oblate state at $I^\pi = 99/2^-$ (encircled in Fig. 7).

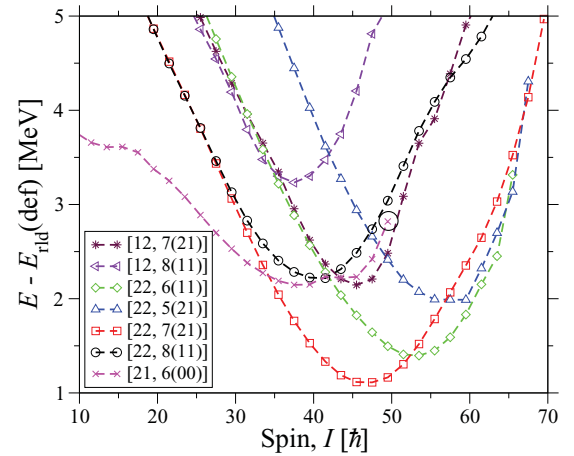


FIG. 7. (Color online) Calculated excitation energies E relative to those of a rotating liquid drop E_{rld} as a function of spin of six low-energy configurations with $(\pi, \alpha) = (-, 1)$ corresponding to $\varepsilon_2 \approx 0.32$ and $\gamma \approx 5^\circ$ and for the less collective [21,6(00)] configuration which terminates in a noncollective state ($\gamma = 60^\circ$) at $I^\pi = 99/2^-$ (encircled).

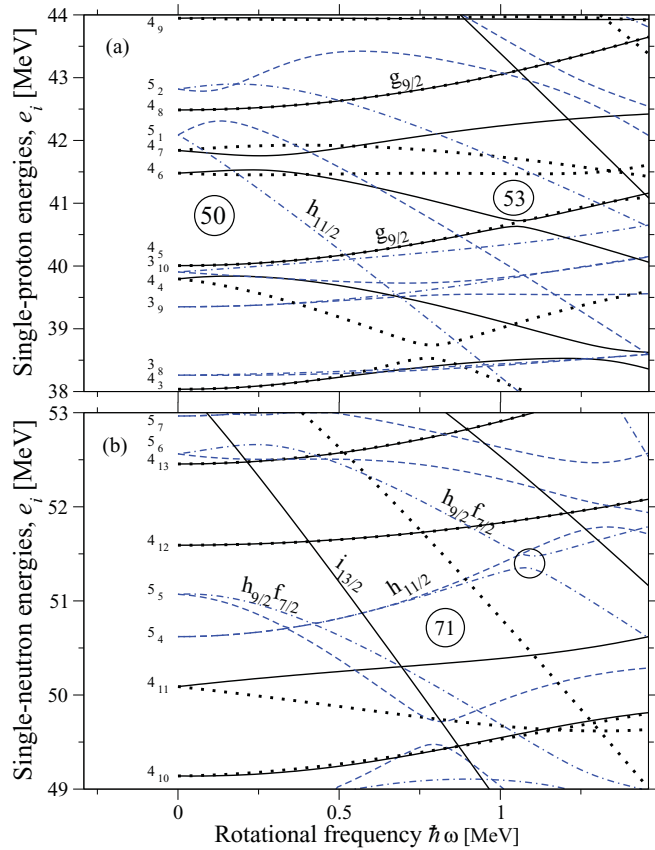


FIG. 8. (Color online) Single-particle proton (a) and neutron (b) energies in the rotating frame (Routhians) as a function of rotational frequency at a deformation of $\varepsilon_2 \approx 0.32$, $\gamma \approx 5^\circ$. The orbitals are labeled at $\hbar\omega = 0$ by the oscillator quantum number N with the ordering within the N shell as a subscript. A few orbitals which are important for the present interpretation are labeled by their dominant j shell(s). The lines distinguish between different parity and signature (π, α) combinations: solid lines represent $(+, +1/2)$, dotted lines $(+, -1/2)$, dashed lines $(-, +1/2)$, and dash-dotted lines $(-, -1/2)$. The area marked with a circle refers to the crossing discussed in the text.

To understand the single-particle occupancy for the configurations with large deformation, the relevant Routhians are plotted for protons and neutrons for $\varepsilon_2 \simeq 0.32$, $\gamma \simeq 5^\circ$ in Fig. 8. The favored proton configurations above $\hbar\omega \simeq 0.5$ MeV [see Fig. 8(a)] are the positive-parity configurations

$$\pi(g_{9/2})^{-1}(d_{5/2}g_{7/2})^2(h_{11/2})^2 \quad (\text{or } [12])$$

and

$$\pi(g_{9/2})^{-2}(d_{5/2}g_{7/2})^3(h_{11/2})^2 \quad (\text{or } [22]),$$

where the latter, with two $g_{9/2}$ proton excitations for the same neutron configuration, is calculated to be lower in energy. Therefore, only this proton configuration is of interest for the interpretation of band 6 in ^{125}I and band a in ^{126}Xe .

For neutrons [see Fig 8(b)] starting from the $N = 71$ gap at $\hbar\omega \simeq 0.8$ MeV, the lowest configurations are built with particles in all orbitals below this gap plus one $h_{11/2}$ or $i_{13/2}$ particle or with excitations from $h_{9/2}f_{7/2}$ into these higher- j subshells. Two possible negative-parity neutron configurations

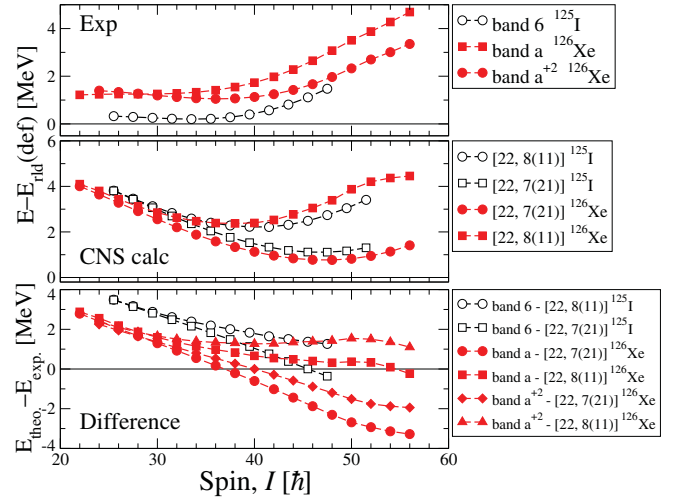


FIG. 9. (Color online) Comparison between the experimentally observed rotational bands in ^{125}I and ^{126}Xe (top panel) and the CNS predictions (middle panel) for the $[22, 8(11)]$ and $[22, 7(21)]$ configurations with $(\pi, \alpha) = (-, 1)$. The bottom panel shows the energy difference between theory and observation. For ^{126}Xe , the energies of band a, lifted by two units in spin and 1178 keV in energy, are included as “band a $^{+2}$ ”.

at this deformation with properties resembling the experimental bands are

$$v[(h_{11/2})^7(h_{9/2}f_{7/2})^2(i_{13/2})^1] \quad (\text{or } [7(21)])$$

and

$$v(h_{11/2})^8[(h_{9/2}f_{7/2})^1(i_{13/2})^1] \quad (\text{or } [8(11)]).$$

These two configurations, combined with the favored proton structure mentioned above, are candidates for the structure of band 6. The other two low-energy configurations, $[22, 5(21)]$ and $[22, 6(11)]$, are ruled out since their calculated minima appear at too high a spin.

In Fig. 9 the calculated energies for the $[22, 7(21)]$ and $[22, 8(11)]$ configurations are compared with those of the experimentally observed bands. The top panel shows the experimental energies of band 6 in ^{125}I and band a in ^{126}Xe relative to the rotating liquid drop energy. The two bands deviate in energy by about 1 MeV over the entire spin range. This is surprising for collective bands, which otherwise have almost identical properties. Furthermore, the ^{126}Xe band reaches relative excitation energies close to 5 MeV at the highest spins, which exceeds typically observed energies by about a factor of 2 [26]. This might raise doubts about the experimental excitation energy and spin assignments. In fact, Ronn Hansen *et al.* [21] suggest that the ^{126}Xe band could be lifted by two units in spin and by 1178 keV in energy. This alternative is included in Fig. 9 as “band a $^{+2}$ ”. However, a large energy difference remains between the bands in the two nuclei, in particular at lower spin.

The calculated energies of the two low-energy configurations which come close to the experimental bands, $[22, 7(21)]$ and $[22, 8(11)]$, are displayed in the middle panel of Fig. 9. They lie close in energy at lower spins, but they start to

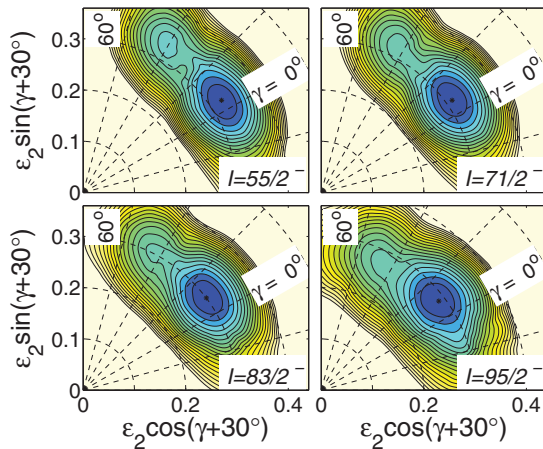


FIG. 10. (Color online) Calculated potential energy surfaces for ^{125}I for the $[22,8(11)]$ configuration in the spin range $I^\pi = 55/2^- - 95/2^-$. The contour line separation is 0.25 MeV.

deviate considerably from each other above $I \simeq 35$. Since the $[22,7(21)]$ configuration appears somewhat lower in energy, it could be considered for the structure of the bands. On the other hand, the general behavior of the experimental curves resembles more closely that of the $[22,8(11)]$ configuration and, therefore, we favor it for the structure of the bands.

In the lower panel of Fig. 9, the difference between calculated and experimental energies is plotted. These differences are large. For the ^{125}I band, the calculated energies for both configurations come reasonably close to experiment only at the highest spins. For the ^{126}Xe band, the energy of the $[22,8(11)]$ configuration is in fair agreement with experiment in this spin range, whereas the $[22,7(21)]$ configuration deviates significantly. Thus, it is concluded that the present CNS calculations are unable to describe the data in a satisfactory way. Similar discrepancies between experiment and calculation have been observed for ^{124}Ba [5], ^{125}Xe [20], and the other high-spin bands in ^{126}Xe [21]. This is difficult to understand considering the successful description of high-spin data within the CNS approach in various regions of the nuclear chart [14,26,29–32] and should be further explored.

Potential energy surfaces for the $[22,8(11)]$ configuration for ^{125}I are displayed in Fig. 10. A deep, stable minimum is observed at $\epsilon_2 \approx 0.32$ and $\gamma \approx 8^\circ$ in the spin range relevant for band 6.

In the upper panel of Fig. 11 the observed spins as a function of transition energy are compared. In ^{126}Xe , at $E_\gamma \simeq 2.4$ MeV, a gain in alignment is observed which is also evident as a discontinuity in the $J^{(2)}$ values at this frequency (see Fig. 4). This can be explained by the crossing of an $h_{11/2}$ with an $h_{9/2}f_{7/2}$ neutron at this frequency [see Fig. 8(b)]. The lower panel shows the calculated spins for the $[22,8(11)]$ configuration for the two nuclei. Although there exists a spin difference between experiment and theory, the general behavior of the curves is similar. In particular, the alignment gain for band a in ^{126}Xe is clearly reproduced. No

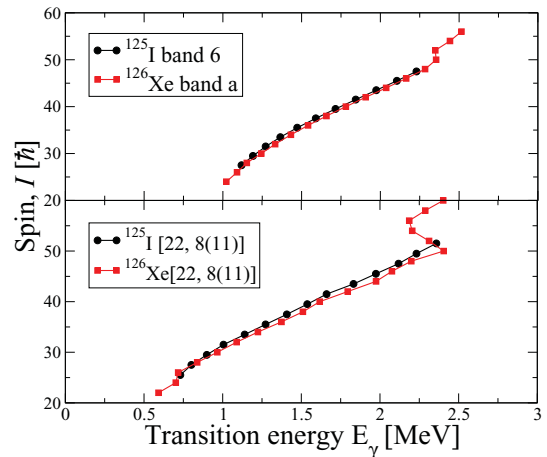


FIG. 11. (Color online) Spins of states plotted as a function of γ -ray energy depopulating these states for ^{125}I and ^{126}Xe . The top panel shows experimental data and the lower panel the results of CNS calculations.

such discontinuity is predicted for the $[22,7(21)]$ configuration by the calculation.

V. SUMMARY

A new rotational band was discovered in ^{125}I in a study with the Gammasphere spectrometer. It consists of eleven $E2$ transitions and forms a regular sequence up to high spin. The band decays into a previously known negative-parity band at $I^\pi = 47/2^-$. The properties of the band are similar to those of the highly deformed bands recently discovered in neighboring nuclei [5,20,21] and it is essentially identical to band a in ^{126}Xe . This suggests that the two bands are associated with similar configurations. However, their excitation energies, relative to the rotating liquid drop energies, differ by $\simeq 1$ MeV, which is surprisingly large for collective bands in neighboring nuclei.

CNS calculations were carried out for both ^{125}I and ^{126}Xe . The properties of none of the configurations expected theoretically at low energy are in satisfactory agreement with those of the new band 6 in ^{125}I and its “identical” partner, band a in ^{126}Xe , and it remains a puzzle why the theoretically expected lowest-energy configurations are not observed experimentally. However, comparisons of various features of the bands with the results of the calculations suggest that the $\pi[(g_{9/2})^{-2}(d_{5/2}g_{7/2})^n(h_{11/2})^2] \otimes \nu[(d_{5/2}g_{7/2})^{-4}(h_{11/2})^8(s_{1/2}d_{3/2})^2(h_{9/2}f_{7/2})^1(i_{13/2})^1]$ configuration with $n = 3$ for band 6 in ^{125}I and $n = 4$ for band a in ^{126}Xe (or $[22,8(11)]$ in the shorthand notation) provides the most straightforward description of the experimental data. The high- j ($h_{11/2}$ and $i_{13/2}$) components in these configurations are in agreement with those previously suggested for band a in ^{126}Xe on the basis of cranked shell-model calculations [21].

ACKNOWLEDGMENTS

The authors thank the ATLAS and Gammasphere operations staff and are grateful to J. P. Greene for preparing

the target. Purnima Singh acknowledges financial assistance from the DST, India, and Somnath Nag the support from CSIR, India, under Contract No. 09/081(0704)/2009-EMR-I. The work was supported by DST, India, under Project No. SR/S2/HEP-09/2005, by the Swedish Science Research

Council, by the German BMBF under Contract No. 06 BN 109, by the Danish FNU Council for Natural Sciences, and by the US Department of Energy, Office of Nuclear Physics, under Contracts No. DE-AC02-06CH11357, No. DE-FG02-94ER40848, and No. DE-AC03-76SF00098.

-
- [1] E. S. Paul, J. Simpson, S. Araddad, C. W. Beausang, M. A. Bentley, M. J. Joyce, and J. F. Sharpey-Schafer, *J. Phys. G* **19**, 913 (1993).
- [2] P. Singh *et al.*, *Phys. Rev. C* **82**, 034301 (2010).
- [3] A. Al Khatib *et al.*, *Eur. Phys. J. A* **36**, 21 (2008).
- [4] A. K. Singh *et al.*, *Phys. Rev. C* **70**, 034315 (2004).
- [5] A. Al Khatib *et al.*, *Phys. Rev. C* **74**, 014305 (2006).
- [6] V. P. Janzen *et al.*, *Phys. Rev. Lett.* **72**, 1160 (1994).
- [7] D. R. LaFosse *et al.*, *Phys. Rev. C* **50**, 1819 (1994).
- [8] V. P. Janzen *et al.*, *Phys. Rev. Lett.* **70**, 1065 (1993).
- [9] D. R. LaFosse, D. B. Fossan, J. R. Hughes, Y. Liang, P. Vaska, M. P. Waring, and J.-Y. Zhang, *Phys. Rev. Lett.* **69**, 1332 (1992).
- [10] K. Starosta *et al.*, *Phys. Rev. C* **64**, 014304 (2001).
- [11] E. S. Paul, H. R. Andrews, V. P. Janzen, D. C. Radford, D. Ward, T. E. Drake, J. DeGraaf, S. Pilotte, and I. Ragnarsson, *Phys. Rev. C* **50**, 741 (1994).
- [12] E. S. Paul *et al.*, *Phys. Rev. C* **59**, 1984 (1999).
- [13] I. Ragnarsson, V. P. Janzen, D. B. Fossan, N. C. Schmeing, and R. Wadsworth, *Phys. Rev. Lett.* **74**, 3935 (1995).
- [14] A. V. Afanasjev, D. B. Fossan, G. J. Lane, and I. Ragnarsson, *Phys. Rep.* **322**, 1 (1999).
- [15] D. Santos *et al.*, *Phys. Rev. Lett.* **74**, 1708 (1995).
- [16] Y.-X. Luo *et al.*, *Z. Phys. A* **329**, 125 (1988).
- [17] E. S. Paul *et al.*, *Phys. Rev. C* **71**, 054309 (2005).
- [18] A. V. Afanasjev and I. Ragnarsson, *Nucl. Phys. A* **608**, 176 (1996).
- [19] R. M. Clark *et al.*, *Phys. Rev. Lett.* **76**, 3510 (1996).
- [20] A. Al Khatib *et al.*, *Phys. Rev. C* **83**, 024306 (2011).
- [21] C. Ronn Hansen *et al.*, *Phys. Rev. C* **76**, 034311 (2007).
- [22] I. Y. Lee, *Nucl. Phys. A* **520**, 641 (1990).
- [23] D. C. Radford, *Nucl. Instrum. Methods A* **361**, 297 (1995).
- [24] T. Bengtsson and I. Ragnarsson, *Nucl. Phys. A* **436**, 14 (1985).
- [25] I. Ragnarsson, *Phys. Lett. B* **264**, 5 (1991).
- [26] B. G. Carlsson and I. Ragnarsson, *Phys. Rev. C* **74**, 011302(R) (2006).
- [27] J.-Y. Zhang, N. Xu, D. B. Fossan, Y. Liang, R. Ma, and E. S. Paul, *Phys. Rev. C* **39**, 714 (1989).
- [28] K. Pomorski and J. Dudek, *Phys. Rev. C* **67**, 044316 (2003).
- [29] I. Ragnarsson, *Nucl. Phys. A* **557**, 167c (1993).
- [30] A. O. Evans *et al.*, *Phys. Rev. Lett.* **92**, 252502 (2004).
- [31] J. J. Valiente-Dobón *et al.*, *Phys. Rev. Lett.* **95**, 232501 (2005).
- [32] J. Gellanki *et al.*, *Phys. Rev. C* **80**, 051304(R) (2009).